Journal of Inclusion Phenomena and Molecular Recognition in Chemistry 9: 91–99, 1990.

Influence of Template on Crystallization of ZSM-5 Zeolites

P. N. JOSHI*, G. N. RAO, A. N. KOTASTHANE, and V. P. SHIRALKAR
National Chemical Laboratory, Pune 411008, India

(Received 28 November 1988; in final form 7 August 1989)

Abstract. Pentasil zeolites of ZSM-5 type are synthesised hydrothermally using triethyl-*n*-proplyammonium bromide (TEPA-Br) and triethyl-*n*-butylammonium bromide (TEBA-Br). The crystallization kinetics, followed by XRD, SEM and thermal analysis, clearly demonstrate the influence of size and molecular weight of the templating quaternary ammonium cation (QAC) species on the rates of nucleation and crystallization. The values of the apparent activation energies for nucleation and crystal growth indicate that both nucleation and crystal growth are faster when TEPA-Br rather than TEBA-Br is used as a template. The quantitative identification of intergrown phases characterizes both the phases to be ZSM-5 zeolite. Thermoanalytical curves for both these zeolites in as-synthesised forms exhibit two-step oxidative decomposition of the occluded organic species. This suggests that the quaternary ammonium cation may be located at two energetically different sites within the zeolite channels. The equilibrium sorption capacity, however, is found to increase in the order of size and molecular weight of the templating species in both the zeolites. The nature of acid site distribution, obtained from the temperature programmed desorption of ammonia is found to be independent of the templating species used during the synthesis.

Key words. Zeolite, ZSM-5, synthesis, crystallization.

1. Introduction

Zeolite ZSM-5 was first synthesized [1, 2] using tetra-*n*-propylammonium cation as a template. Recently, it has been shown that this zeolite can be synthesized using different quaternary ammonium cations (such as TEPA-Br, TEBA-Br) [3, 4] amines [5], and alcohols [6]. In each of these studies, it was shown that high purity ZSM-5 can be synthesised and in some cases the kinetics of crystallization are discussed in terms of the applicability of the Avrami–Erofeev equation [7] and evaluation of apparent activation energies for the process of nucleation and crystal growth. Under identical gel composition and synthesis conditions it is found [3, 4] that the change in templating species affects the rates of nucleation and crystallization. Even the region of metastability of ZSM-5 crystallization is found to be affected drastically by the template and templating becomes operative only in the environment of the right gel chemistry [8, 9]. It was therefore of interest to synthesize ZSM-5 zeolite using triethyl-*n*-propylammonium bromide (TEPA-Br) and triethyl-*n*-butylammonium bromide (TEBA-Br) as templates. The results of the kinetics of the zeolite synthesis along with the influence of temperature and of the type of templating cation thereon are reported here. The influence of the change in the templating species on the structural and the sorption properties of the synthesized zeolites is also discussed.

*Author for correspondence.
NCL communication No. 4903.

2. Experimental

Synthesis experiments were carried out in stainless steel autoclaves of capacity 275 mL under static (unstirred) conditions in the temperature range of 433–473 K. A fixed gel composition $3.36\,R_2O : 25.4\,Na_2O : Al_2O_3 : 85\,SiO_2 : 3200\,H_2O$ (where R = TEPA or TEBA) was employed during the crystallization kinetics experiments. The reagent materials we used were sodium silicate ($SiO_2 = 27.2\%$, $Na_2O = 8.4\%$, $H_2O = 63.9\%$), $Al_2(SO_4)_3 \cdot 16\,H_2O$ (Loba Chemie), sulphuric acid, 98% (AnalaR grade BDH) and tetraalkylammonium compounds TEPA-Br and TEBA-Br (synthesized in our laboratory). In a typical experiment 40.0 g of sodium silicate was diluted with 30 mL of deionized water. To it was added 3.42 g of TEBA-Br (or 3.22 g of TEPA-Br) dissolved in 20 mL deionized water. To this mixed solution was added a solution of 1.35 g $Al_2(SO_4)_3 \cdot 16\,H_2O$ dissolved in 50 mL of water and 3.52 g of sulphuric acid. The gel was maintained at the crystallization temperature for various lengths of time. The products were filtered, washed with distilled water, dried at 393 K, and finally were calcined at 823 K for 10 h to obtain the sodium form. The chemical composition of the fully crystalline ZSM-5 was estimated by wet chemical analysis, atomic absorption and flame photometry. X-ray diffraction patterns on powder samples were collected on a Philips PW 1730 using Ni filtered CuK_α radiation. The percentage crystallinity was estimated [10] from the ratio of peak area between 2θ – 22–25° of the product and that of the reference sample of best crystallinity of the present studies.

The crystal size and habit of the crystalline phases were examined by a scanning electron microscope (Stereoscan Model 150 UK). The samples were coated with an evaporated Au–Pd film. The IR spectra of the samples were recorded with a Perkin-Elmer 221 Spectrometer using the Nujol mull technique. KCN was used as an internal standard using 2200 cm^{-1} as the reference peak. A high vacuum gravimetric adsorption system with a McBain balance was used for the measurements of sorption properties with water, cyclohexane and *n*-hexane as probe adsorbates. DTG and DTA curves were recorded simultaneously on an automatic (MOM, Budapest, Hungary, Type OD-102) derivatograph described by Paulick *et al.* [11]. The specific surface area of the samples were determined by low temperature (78 K) sorption of nitrogen using the conventional BET technique.

3. Results and Discussion

The crystallization kinetics in the reaction temperature range 433–473 K of the synthesis of ZSM-5 with the oxide mole ratio $3.36\,R_2O : 25.4\,Na_2O : Al_2O_3 : 85\,SiO_2 : 3200\,H_2O$ using $R = TEBA^+$ or $TEPA^+$ are shown in Figure 1. The curves exhibit a typical sigmoid nature characteristic of two distinct stages [3, 4]: (a) an induction or nucleation period when nuclei are formed, and (b) a crystal growth period when nuclei grow into crystals. If it is assumed that the rate of nucleation is inversely proportional to the induction period, then it is evident from the figure that the rate of nucleation decreases as the crystallization temperature decreases. It is also clear from the figure that the rate of crystal growth increases

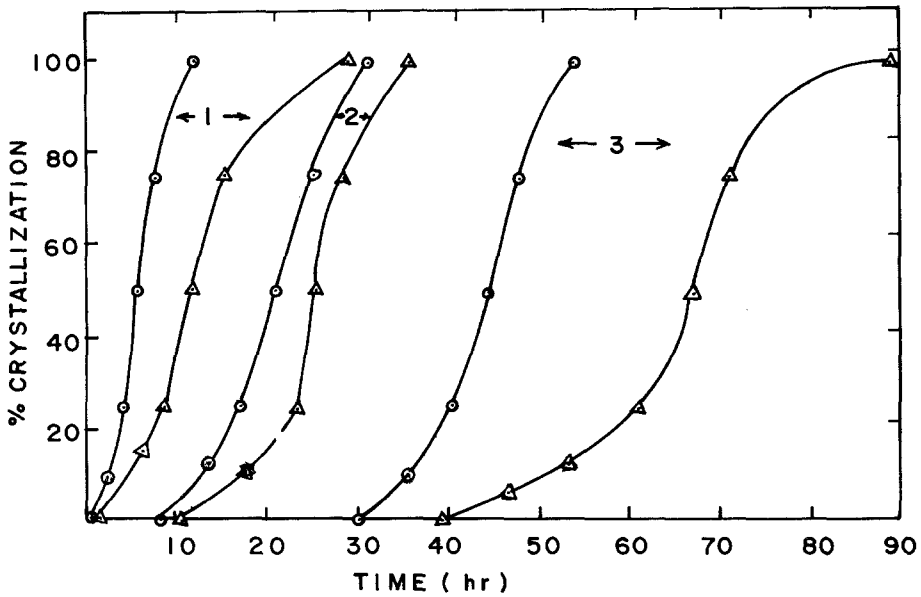

Fig. 1. Crystallization kinetics of ZSM-5 zeolites using (⊙) TEPA-Br and (△) TEBA-Br at (1) 473 K, (2) 453 K and (3) 433 K.

with crystallization period, passes through maximum at 40–60% of the total crystallinity followed by a decrease while approaching to 100% crystallinity. The maximum in the rate of crystal growth increases as the temperature increases. Crystallization curves from Figure 1 thus clearly demonstrate the considerable influence of the reaction temperature on the kinetics of the process. The higher rate of nucleation and crystal growth at higher reaction temperature suggests the enhanced solubility of the aluminosilicate gel on increasing the crystallization temperature which exerts a beneficial effect on the crystallization process.

Figure 1 clearly shows that at the given crystallization temperature faster nucleation and crystallization are achieved when TEPA-Br is used as the template. It is expected that the kinetics of high silica crystallization is a complex function of many variables including the source of the organic template. The larger size of TEBA-Br compared to the TEPA-Br species may be operative in the slower rate

Table I. Avrami–Erofeev parameters for ZSM-5 synthesis.

Synthesis Temperature K	TEBA-Br	System	TEPA-Br	System
	10^2k	m	10^2k	m
433	1.5	7.8	2.5	4.9
453	4.0	4.5	6.1	3.5
473	8.2	2.0	15.1	1.8

of arranging polysilicate ions around it and thus may be responsible for the slower rate of nucleation and crystallization.

3.1. KINETICS OF NUCLEATION AND CRYSTALLIZATION

The process of zeolite nucleation and crystallization are usually represented [3, 4] by sigmoid curves (Figure 1) which are described mathematically by the Avrami–Erofeev equation

$$\ln\{1/(1-\alpha)\} = (kt)^m \tag{1}$$

where α and t are the fractional conversion and reaction time, respectively, and k and m are constants. The data of Figure 1 were fitted to Equation (1) and linear plots were obtained. The values of m and k obtained from these linear plots are listed in Table I. The salient feature of Table I is in accordance with the thermodynamic expectation of a decrease in k and an increase in m as the temperature of the zeolite synthesis decreases. The increase in k indicates a faster rate of nucleation and a decrease in m signifies faster crystallization. Table I shows that the values of k obtained when TEPA-Br is used as template are higher than those when TEBA-Br is used. This clearly indicates a faster rate of nucleation in the case of TEPA-Br. Similarly, a lower value of m in the case of TEBA-Br as template than those with TEBA-Br clearly indicates faster crystallization when the former is used as a template. The slower rate of both nucleation and crystallization in the case of TEBA-Br as template is probably due to the comparatively larger size of TEBA-Br compared to TEPA-Br.

Assuming that the formation of the nuclei during the induction period is an energetically activated process, the apparent activation energy for nucleation E_n was calculated from the temperature dependence of the rate of nucleation. The rate of crystallization was obtained from the point of inflection in the crystallization curve. Figure 2 shows the linear plots obtained by applying the Arrhenius equation to the crystallization curves. E_n and E_c values derived from these plots are summarised in Table II. The E_n values for synthesis of zeolite using both the templates are almost identical (118 kJ, mol^{-1}). The value of E_c for the TEBA-Br system (78.6 kJ mol^{-1}) is lower than that of the TEPA-Br system (89.8 kJ mol^{-1}). Since these are apparent and not true values of E_n and E_c and they are functions of many synthesis parameters including synthesis time, temperature, pH, source of raw materials, etc., no meaningful conclusions could be drawn regarding the rates of nucleation and crystallization. However, these values of E_n and E_c are in general agreement with values reported earlier in the literature [2, 10].

Table II. Apparent activation energies for nucleation and crystallization.

Source of organic	E_n kJ mol^{-1}	E_c kJ mol^{-1}
TEBA-Br	118.1	78.6
TEPA-Br	117.2	89.8

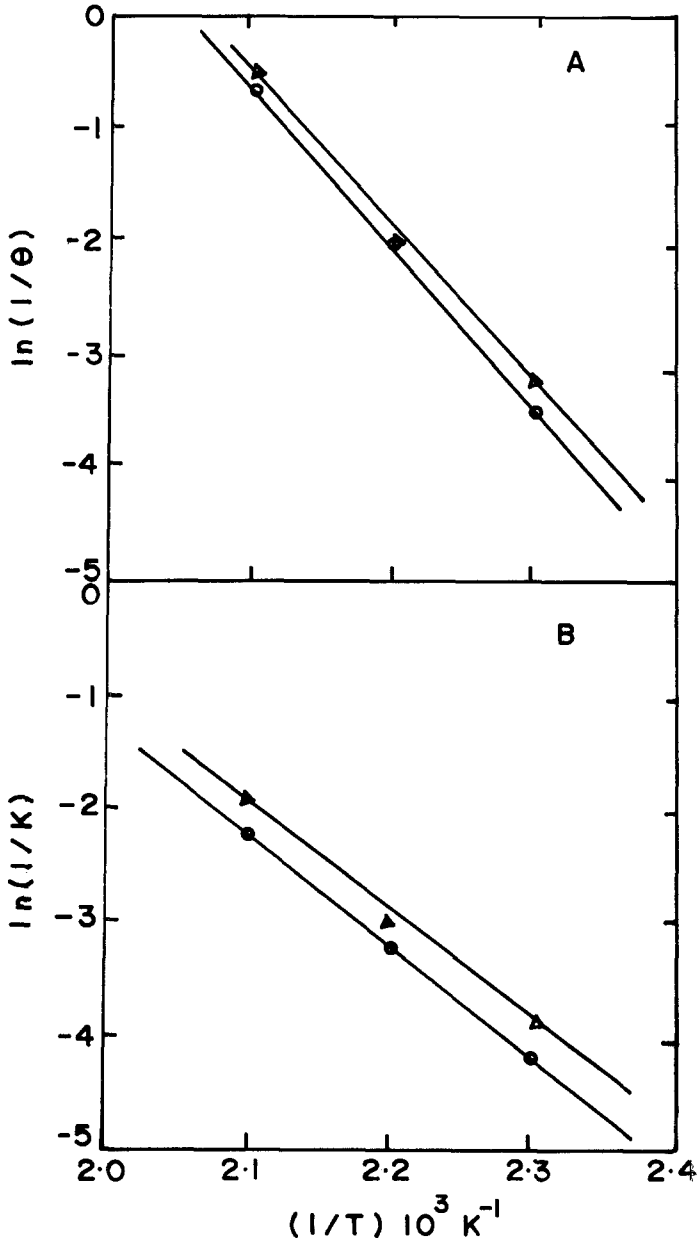

Fig. 2. Arrhenius plots for (a) crystallization and (b) nucleation at 473 K, 453 K, 433 K with (●) TEPA-Br and (▲) TEBA-Br as templates.

3.2. THERMAL ANALYSIS

The DTA curves obtained on the as-synthesised samples using both the templates are shown in Figure 3. Both the DTA curves in the figure exhibit an endothermic effect with a minimum at 373–383 K and a very strong exothermic effect in the temperature range 623–773 K with two pronounced maxima around 683 K and 743 K. The low temperature endotherm is a consequence of the dehydration of the physically sorbed water from zeolite cavities. Organic templating cations are probably ionically bonded [12, 13] to the AlO_4 tetrahedra during hydrothermal crystallization and are stabilized to such an extent that they decompose only at higher temperature on calcination. The exothermic peaks around 683 K and 743 K

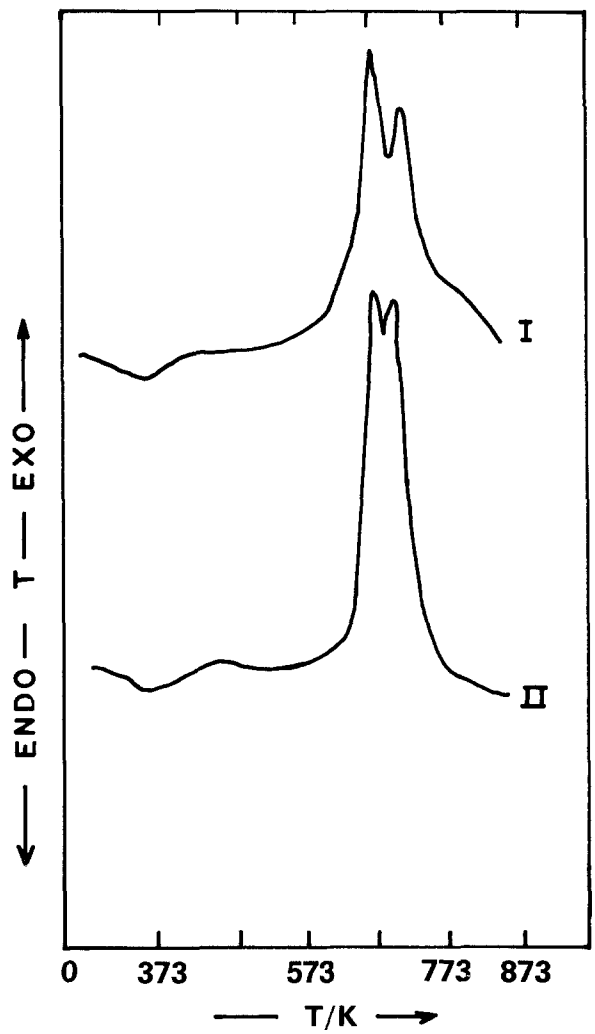

Fig. 3. DTA curves for as-synthesised ZSM-5 zeolites with (I) TEPA-Br and (II) TEBA-Br as template.

on the DTA curves reflect the oxidative decomposition of the templating species in two steps [13, 14]. These organic cations are located at the channel intersection where they interact with the framework negative charges. Therefore the positions of the maxima on the DTA are related to the localization of these organic cations. Two DTA maxima suggest two types of binding of the templates (1) those weakly bonded or occluded in the channels acting as structure directing species and decomposing at comparatively lower temperatures (683 K) and (2) associated with acid sites, i.e. charge compensating on AlO_4 tetrahedra, and decomposing at higher temperature (743 K). The total weight loss obtained from TG in the case of the TEBA-Br system, as expected, was higher (14.5%) than that in the case of the TEPA-Br (12.0%) system.

3.3. SORPTION PROPERTIES

Equilibrium sorption capacities in both the zeolite systems for water and for cyclohexane at 298 K and $P/P_0 = 0.5$ are listed in Table III along with BET surface areas. Higher equilibrium sorption capacities of water (8.2%) and cyclohexane (7.1%) indicates increased void volume in the case of TEBA-Br as a template. The marginal difference in the equilibrium sorption capacity may therefore be due to the difference between the size of the templating molecules and hence pore filling potential. Both zeolites are synthesized at the same temperature (453 K). Therefore indirectly templating species are influencing the sorption capacity. Similar observations are reported by Nayak and Rickert [15].

Table. III. Equilibrium sorption capacities at 25°C and $p/p_0 = 0.5$.

Zeolite sample	Adsorption (g 100 g^{-1} zeolite)		Surface area (BET) $m^2 g^{-1}$
	H_2O	C_6H_{12}	
H/TEPA-Br	7.2	5.5	430*
H/TEBA-Br	8.2	7.1	443*

*N. R. Meshram: *J. Chem. Tech. Biotech.* **37**, 111 (1987)

3.4. IR SPECTRA AND AMMONIA TPD CURVES

Framework IR spectra in the region 400–1300 cm^{-1} obtained for both the zeolites are almost identical. This indicates that the framework IR spectra of fully crystalline material obtained by crystallizing the same gel composition are independent of the templating species used during synthesis. Similarly the strength of the acid site distribution obtained from temperature programmed desorption of ammonia is also found to be independent of the templating species used during synthesis.

3.5. SCANNING ELECTRON MICROGRAPHY (SEM)

It is usually found [16] that different templating species give rise to variation in crystalline habits and crystallite size. The change in source of SiO_2, Al_2O_3 and

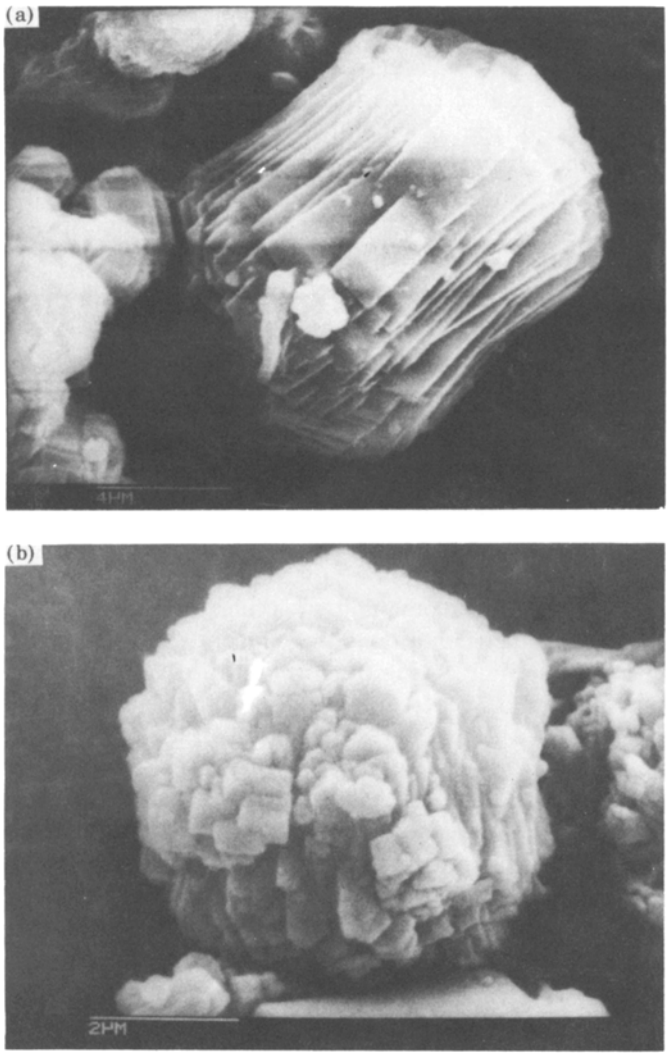

Fig. 4. SEM micrographs of ZSM-5 obtained with (a) TEPA-Br and (b) TEBA-Br at 453 K.

Na_2O also affects the crystallization kinetics and hence affects the habit and size of the crystalline phase. The increase in SiO_2/Al_2O_3 ratio in the gel composition is found [4] to increase the crystallite size. In the present studies the SiO_2/Al_2O_3 ratio and ingredient sources are essentially the same, the SEM photographs in Figure 4 show that the zeolite synthesized with TEBA-Br gives intergrown spherical crystals of 5–6 μm and that synthesized with TEPA-Br gives nearly spherical crystals of 7–8 μm with intergrown layers.

References

1. R. J. Argauer and G. R. Landolt: *U.S. Pat.* 3,702,886 (1972)
2. A. Erdem and L. B. Sand: *J. Catal.* **60**, 241 (1979).

3. S. B. Kulkarni, V. P. Shiralkar, A. N. Kotasthane, R. B. Borade and P. Ratnasamy: *Zeolites* **2**, 313 (1982).
4. A. N. Kotasthane, V. P. Shiralkar, S. G. Hedge and S. B. Kulkarni: *Zeolite* **6**, 253 (1986).
5. Z. Gabelica, M. Cavez-Bierman, P. Boudart, A. Gourgue and J. B. Nagy: *Zeolite Synthesis, Structure, Technology and Applications*, Studies in Surface Science and Catalysis, 24, B. Drzaj, S. Hocevar and S. Pejovnik, Eds., Elsevier, New York, 1985. p. 55.
6. E. Narita, K. Sato and T. Okabe: *Chem. Lett.* 1055 (1984).
7. M. Avrami: *J. Chem. Phys.* **9**, 177 (1941) and B. V. Erofeev, *C.R. Acad. Sci., U.S.S.R.* **52**, 511 (1946).
8. Z. Gabelica, N. Blom and E. G. Derouane: *Appl. Catal.* **5**, 227 (1983).
9. B. M. Lok, T. R. Cannan and C. A. Messina: *Zeolites* **3**, 282 (1983).
10. K. J. Chao, T. C. Tasi, M. S. Chen and I. Wang: *J. Chem. Soc. Faraday Trans. 1* **77**, 547 (1981).
11. F. Paulik, J. Paulik and L. Erdey: *Talanta* **13**, 1405 (1946).
12. K. J. Chao: *Proc. Natl. Sci. Counc., ROC*, **3**, 233 (1979).
13. D. M. Biddy, N. B. Milestone and L. P. Aldridge: *Nature (London)* **285**, 30 (1980).
14. A. N. Kotasthane and V. P. Shiralkar: *Thermochim. Acta* **102**, 37 (1986).
15. V. S. Nayak and L. Riekert: *Acta Phys. Chem.* **31**, 157 (1985).
16. R. Mostovich and L. B. Sand: *Zeolites* **2**, 143 (1982).